NJC

Accepted Manuscript

This is an *Accepted Manuscript*, which has been through the Royal Society of Chemistry peer review process and has been accepted for publication.

Accepted Manuscripts are published online shortly after acceptance, before technical editing, formatting and proof reading. Using this free service, authors can make their results available to the community, in citable form, before we publish the edited article. We will replace this *Accepted Manuscript* with the edited and formatted *Advance Article* as soon as it is available.

You can find more information about *Accepted Manuscripts* in the Information for Authors.

Please note that technical editing may introduce minor changes to the text and/or graphics, which may alter content. The journal's standard Terms & Conditions and the Ethical guidelines still apply. In no event shall the Royal Society of Chemistry be held responsible for any errors or omissions in this *Accepted Manuscript* or any consequences arising from the use of any information it contains.

ROYAL SOCIETY OF CHEMISTRY

www.rsc.org/njc

A fluorescent probe (**NBDTe**) based on an NTe_2 chelating motif has been developed for Hg^{2+} detection.

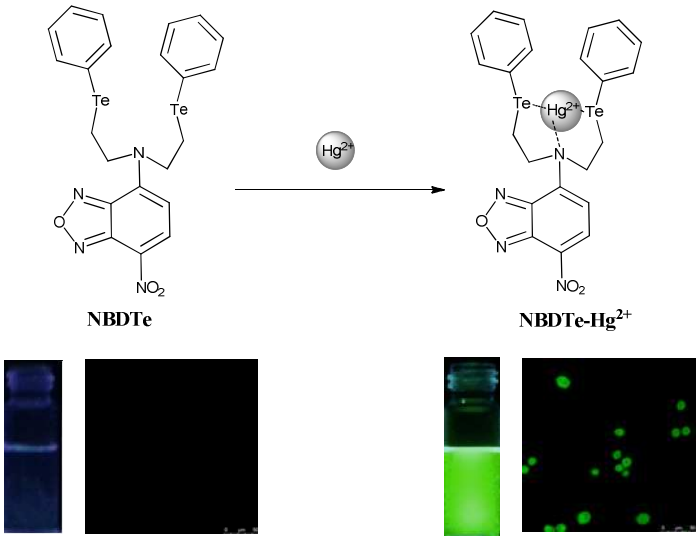

NBDTe **NBDTe-Hg^{2+}**

A highly selective fluorescent sensor for Hg(II) based on an NTe_2 chelating motif and its application to living cell imaging

Shao-Lun Kao, Parthiban Venkatesan and Shu-Pao Wu*

Department of Applied Chemistry, National Chiao Tung University, Hsinchu, Taiwan 300, Republic of China

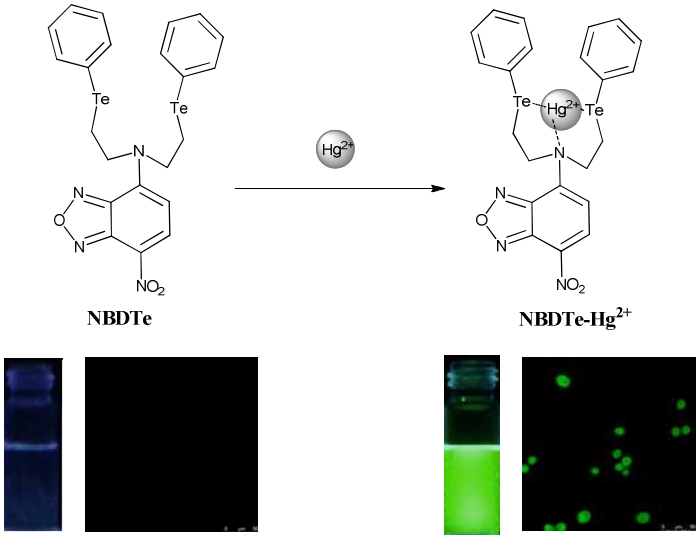

NBDTe **NBDTe-Hg^{2+}**

* Corresponding author. Tel.: +886-3-5712121-ext 56506; fax: +886-3-5723764; e-mail: spwu@mail.nctu.edu.tw

Abstract

A fluorescent probe (**NBDTe**) based on an NTe_2 chelating motif has been developed for the highly selective and sensitive detection of Hg^{2+}. Significant fluorescence enhancement was observed with the chemosensor **NBDTe** in the presence of Hg^{2+}. Moreover, the metal ions Ag^{+}, Al^{3+}, Ca^{2+}, Cd^{2+}, Co^{2+}, Cu^{2+} ,Cr^{3+}, Fe^{2+}, Fe^{3+}, Hg^{2+}, Mg^{2+}, Mn^{2+}, Ni^{2+}, Pb^{2+}, and Zn^{2+} produced only minor changes in the fluorescence values of the system. The association constant (K_a) of Hg^{2+} binding to the chemosensor **NBDTe** was found to be 3.81×10^3 M^{-1}, with a detection limit of 4.2 μM. The maximum fluorescence enhancement caused by Hg^{2+} binding to the chemosensor **NBDTe** was observed over the pH range of 4.0 ~ 10.0. In addition, fluorescence microscopy experiments showed that the chemosensor **NBDTe** can be used as a fluorescent probe for detecting Hg^{2+} in living cells.

Introduction

The development of fluorescent chemosensors for detecting heavy-transition metal ions, such as Fe^{3+}, Cu^{2+}, Cd^{2+}, Hg^{2+}, Pb^{2+},and Zn^{2+} has been an important research topic [1-2]. Among these metal ions, mercury in particular is considered to be a toxic heavy metal element. Three forms of mercury exist, such as inorganic mercury, alkylmercury, and elemental mercury [3]. Mercury pollution occurs through various routes, such as mining and the incineration of fossil fuel and solid waste [4]. Mercury ions can bind the thiol groups in proteins, leading to cell malfunction and subsequently triggering several health problems in the brain, kidney, and central nervous system. Cellular accumulation of mercury can result in a wide variety of diseases, such as prenatal brain damage, serious cognitive and motion disorders, and Minamata disease [5]. Owing to its extreme toxicity, the United States Environmental Protection Agency (EPA) has established the standard for the maximum allowed level of mercury in dietary and environmental sources to be 2 ppb (10 nM).

Several methods for the detection of mercury in various samples have been developed, including atomic absorption/emission spectroscopy [6], inductively coupled plasma-mass spectroscopy (ICPMS) [7], inductively coupled plasma-atomic emission spectrometry (ICP-AES) [8], and voltammetry [9]. Recently, more attention has been focused on the development of fluorescent chemosensors for the detection of Hg^{2+} ions [10-20].

Hg^{2+} is known to be a fluorescence quencher through spin–orbit coupling [21]. Owing to their sensitivity, fluorescent chemosensors that detect metal ions by fluorescence enhancement are more easily monitored than those that detect by fluorescence quenching. This paper reports on a newly designed NBD-based fluorescence enhancement chemosensor for Hg^{2+}, which operates on photoinduced electron transfer (PET). The binding of Hg^{2+} to the chemosensor blocks the PET

mechanism and greatly enhances the fluorescence of NBD.

In this work, we designed an NBD-based fluorescent chemosensor for metal-ion detection. Two parts make up the chemosensor **NBDTe**: an NBD moiety as a reporter and bis(2-(phenyltellanyl)ethyl)amine units as a metal ion chelator (Scheme 1). **NBDTe** exhibits weak fluorescence due to quenching by photoinduced electron transfer from the lone-pair electrons on the tellurium atom to NBD. The binding of metal ions to the chemosensor blocks the PET mechanism and results in considerable fluorescence enhancement of NBD. The metal ions Ag^{+}, Al^{3+}, Ca^{2+}, Cd^{2+}, Co^{2+}, Cu^{2+} ,Cr^{3+}, Fe^{2+}, Fe^{3+}, Hg^{2+}, Mg^{2+}, Mn^{2+}, Ni^{2+}, Pb^{2+}, and Zn^{2+} were tested for metal-ion-binding selectivity with **NBDTe**, but Hg^{2+} was the only ion that caused green emission upon binding.

Results and discussion

The chemosensor **NBDTe** was synthesized through the reaction of bis(2-(phenyltellanyl)ethyl)amine and 4-chloro-7-nitrobenzo-2-oxa-1,3-diazole at room temperature (Scheme 1). After the reaction, the mixture was extracted with dichloromethane to remove the salt, then purified by column chromatography (eluting with DCM) with an **NBDTe** yield of 30%. The chemosensor **NBDTe** is red and has an absorption band centered at 490 nm. The chemosensor **NBDTe** exhibits weak fluorescence (Φ = 0.002) due to photoinduced electron transfer from the lone-pair electrons on the tellurium atom to the NBD moiety.

The sensing ability of **NBDTe** was tested by mixing it with the metal ions Ag^{+}, Al^{3+}, Ca^{2+}, Cd^{2+}, Co^{2+}, Cu^{2+}, Cr^{3+}, Fe^{2+}, Fe^{3+}, Hg^{2+}, Mg^{2+}, Mn^{2+}, Ni^{2+}, Pb^{2+}, and Zn^{2+}. Qualitatively, Hg^{2+} was the only ion that caused a change in the color (from red to yellow) of the **NBDTe** solution and green fluorescence from **NBDTe** (Fig. 1). The other metal ions had no significant effect on the fluorescence of **NBDTe**. Quantitative

fluorescence spectra of **NBDTe** were recorded in the presence of several transition-metal ions. Hg^{2+} was the only metal ion that caused significant green emission (Fig. 2). During the titration of **NBDTe** against Hg^{2+}, a new emission band centered at 525 nm was observed (Fig. 3). After the addition of 5 equivalents of Hg^{2+}, the emission intensity reached a maximum. The quantum yield of the emission band was $\Phi = 0.086$, which is 43 times higher than that of **NBDTe**, with $\Phi = 0.002$. These results indicate that Hg^{2+} is the only metal ion that readily binds to **NBDTe**, causing significant fluorescence enhancement and permitting the highly selective detection of Hg^{2+}.

To study the influence of other metal ions on the binding of Hg^{2+} to **NBDTe**, we performed competitive experiments with mixtures of Hg^{2+} (150 μM) and other metal ions (150 μM; Fig. 4). The fluorescence enhancement observed for most of the mixtures of Hg^{2+} with other metal ions was similar to that caused by Hg^{2+} alone. Reduced fluorescence enhancement was observed when Hg^{2+} was mixed with Cd^{2+} or Ag^{+}. This indicates that only Cd^{2+} and Ag^{+} compete with Hg^{2+} for binding with **NBDTe**. Most of the other metal ions do not interfere with the binding of **NBDTe** to Hg^{+}.

The binding stoichiometry of the **NBDTe**-Hg^{2+} complex was determined using Job plot experiments. In Fig. 5, the emission intensity at 525 nm is plotted against the molar fraction of chemosensor **NBDTe** under a constant total concentration. The maximum intensity was reached when the molar fraction was 0.5. This result indicates a 1:1 ratio for the **NBDTe**-Hg^{2+} complexes. The formation of an **NBDTe**-Hg^{2+} complex was also confirmed by ESI-MS, in which the peak at $m/z = 890.1$ indicated a 1:1 stoichiometry for the **NBDTe**-Hg^{2+} complex (see Figure S7 in the supplementary material). The association constant K_a was evaluated graphically by plotting $1/(F-F_0)$ against $1/[Hg^{2+}]$ (Fig. 6). The data was linearly fit according to the

Benesi–Hilderbrand equation, and the K_a value was obtained from the slope and intercept of the line. The K_a value of the **NBDTe**-Hg^{2+} complex was 3.81×10^3 M^{-1}. The detection limit of **NBDTe** as a fluorescent sensor for the analysis of Hg^{2+} was determined from the plot of fluorescence intensity as a function of the concentration of Hg^{2+} (see Figure S8 in the supporting information). **NBDTe** was found to have a detection limit of 4.2 μM, which is reasonable for the detection of micromolar concentrations of Hg^{2+}.

To gain a clearer understanding of the structure of the **NBDTe**–Hg^{2+} complex, ^1H NMR spectroscopy (Fig. 7) was employed. Hg^{2+} is a heavy metal ion and can affect proton signals that are close to the Hg^{2+} binding site[11]. ^1H NMR spectra of **NBDTe** recorded with increasing amounts of Hg^{2+} showed that the proton (H_d) signal at δ = 3.2 ppm shifted downfield and the proton (Hc) signal at δ = 4.3 ppm shifted upfield as Hg^{2+} was added. The proton signal H_e from the benzene ring was slightly affected by the binding of Hg^{2+}. These observations show that Hg^{2+} binds to **NBDTe** through one nitrogen and two tellurium atoms.

A pH titration of **NBDTe** was carried out to determine a suitable pH range for Hg^{2+} sensing. As depicted in Fig. 8, the emission intensities of metal-free **NBDTe** are very low at all pH values. After mixing **NBDTe** with Hg^{2+}, the emission intensity at 525 nm increased in the pH range of 4.0–10.0. These observations reveal that the **NBDTe**–Hg^{2+} complex is essentially pH-insensitive over the range of 4.0 to 10.0, indicating that the fluorescence of the **NBDTe**–Hg^{2+} complex is stable over a wide pH range.

To investigate the mechanism of Hg^{2+}-detection, density functional theory (DFT) calculations were employed using the Gaussian 09 software package. As shown in Scheme 2, the highest occupied molecular orbital (HOMO) of the NTe_2 moiety (electron donor) is close to that of the fluorophore NBD (electron acceptor); the

HOMO energy level (−5.96 eV) of the NTe_2 moiety is higher than that of NBD (−6.52 eV). Consequently, when the NBD moiety is excited by light, electron transfer from the NTe_2 moiety to the NBD moiety is energetically allowed. Hence, the NBD fluorescence is quenched by the PET process ($\Phi < 0.01$). In contrast, upon the binding of **NBDTe** to Hg^{2+}, the HOMO energy level of the NTe_2 moiety decreases to below that of NBD; the PET process is thus forbidden and NBD fluorescence reemerges.

In order to investigate Hg^{2+} binding to **NBDTe**, density functional theory (DFT) calculations were also employed. Due to the 1:1 ligand-to-metal complex determined by the Job plot measurements, the chemosensor **NBDTe** with and without Hg^{2+} was subjected to energy optimization at the B3LYP hydrid functional with the LanL2DZ basis set. The lowest energy conformation for **NBDTe**-Hg^{2+} has one chemosensor **NBDTe** molecule binding with one Hg^{2+} ion, where the Hg^{2+} ion is bonded by one nitrogen and two tellurium atoms at a distance of 2.6, 2.9, and 2.9 Å, respectively (Fig. 9).

The reversibility of a chemosensor to target ion binding is a very important feature in practical applications. The reversibility of Hg^{2+} binding to **NBDTe** was therefore investigated. This was verified by the introduction of S^{2-}, which has a strong binding ability towards the thiophilic Hg^{2+}. Fig. 10 shows that the introduction of S^{2-} can immediately restore the initial non-fluorescent state. This regeneration indicates that **NBDTe** can be reused with proper treatment.

The potential of **NBDTe** for imaging Hg^{2+} in living cells was investigated next. First, an MTT assay with a RAW 264.7 cell line was used to determine the cytotoxicity of **NBDTe**. In Fig. 11, the cellular viability was estimated to be greater than 80% after 24 h, which indicates that **NBDTe** (< 25μM) has low cytotoxicity. Cell images were further obtained using a confocal fluorescence microscope. When RAW 264.7 cells were incubated with **NBDTe** (10 μM), no fluorescence was observed (Fig.

12a). After treatment with Hg^{2+}, bright green fluorescence was observed in the RAW 264.7 cells (Fig. 12b). An overlay of fluorescence and bright-field images showed that the fluorescence signals were localized in the intracellular area, indicating a subcellular distribution of Hg^{2+} and good cell-membrane permeability of **NBDTe**.

Conclusion

In conclusion, we have developed a 7-nitrobenzooxadiazole-based fluorescent chemosensor for Hg^{2+} sensing, which exhibits a turn-on response both in vitro and in live cells. This probe displays high selectivity and sensitivity towards Hg^{2+} over other metal ions in aqueous solutions. Most importantly, the chemosensor **NBDTe** can potentially be applied in the fluorescence imaging of living cells. This 7-nitrobenzooxadiazole-based chemosensor **NBDTe** has low cytotoxicity and can therefore be applied for detecting Hg^{2+} in living cells.

Experimental

Materials and Instrumentations.

All solvents and reagents were obtained from commercial sources and used as received without further purification. UV/Vis spectra were recorded on an Agilent 8453 UV/Vis spectrometer. IR data were obtained on Bomem DA8.3 Fourier-Transform Infrared Spectrometer. NMR spectra were obtained on a Bruker DRX-300 NMR and Varian Unity INOVA-500 NMR spectrometer. Fluorescence spectra were recorded in a Hitachi F-4500 spectrometer. Fluorescent images were taken on a Leica TCS SP5 X AOBS Confocal Fluorescence Microscope.

Synthesis of bis(2-(phenyltellanyl)ethyl)amine

1,2-Diphenylditelluride (827.78 mg, 2 mmol) and sodium hydroxide (800 mg, 20 mmol) were dissolved in ethanol (30 mL). Under N_2 atmosphere, $NaBH_4$ (105.9 mg,

2.8 mmol) was added to the mixture. The reaction mixture was stirred at room temperature for 2 h. Then bis(2-chloroethyl)amine (178 mg, 1 mmol) was added to the reaction mixture. The mixture was stirred at 80 ℃ for 5 hr. The solvent was removed under reduced pressure. The residue was dissolved in CH_2Cl_2 (50 mL) and water (100 mL). Organic phase was extracted with CH_2Cl_2 and dried over anhydrous $MgSO_4$. The solvent was evaporated under reduced pressure, and the crude product was purified by column chromatography (hexane : ethyl acetate = 1:1) to give the compound as a white powder. Yield: 207 mg (25 %). Melting point: 79.5-80.4 ℃. ^{1}H NMR (300 MHz, $CDCl_3$): δ 7.68 (m, 4 H), 7.23 (m, 6 H), 3.03 (m, 8 H), 1.91 (s, 1 H); ^{13}C NMR (75 MHz, $CDCl_3$): δ 138.4, 129.1, 127.5, 111.7, 77.3, 76.7, 49.6, 10.3; MS(EI): m/z (%)= 481.0 (5.6), 404.0 (1.2), 332.9 (6.2) 278.1 (50.9). HRMS(EI) Calcd for $C_{16}H_{19}NTe_2$ 480.9613; found 480.9621.

Synthesis of chemosensor NBDTe

4-Chloro-7-nitrobenzo-2-oxa-1,3-diazole(99 mg, 0.5 mmol), bis(2-(phenyl tellanyl)ethyl)amine (207 mg, 0.5 mmol) and triethylamine were dissolved in 20 mL CH_2Cl_2. The mixture was stirred for 5 hours at room temperature. The resulting mixture was washed with water and extracted with dichloromethane (3×50 mL). Organic layer was collected and concentrated. The product was purified by column chromatography (CH_2Cl_2/hexane, v/v = 1:1) to give compound **NBDTe** as a red solid. Yield: 97 mg (30 %). Melting point: 109.8-110.7 ℃. ^{1}H NMR (300 MHz, $CDCl_3$): δ 8.08 (d, 1 H, J = 9.0 Hz), 7.80 (m, 4 H), 7.30 (m, 6 H), 5.49 (d, 1 H, J = 9.0 Hz), 4.14 (m, 4 H), 3.04 (m, 4 H); ^{13}C NMR (75 MHz, $CDCl_3$): δ 144.6, 143.9, 143.2, 139.5, 135.0, 129.4, 128.6, 122.7, 109.9, 101.0, 77.3, 76.7, 55.8, 29.6; MS (ESI^+): m/z (%)= 645.0 (12.0), 616.9 (53.7), 441.0 (17.5), 381.3 (100) $[M+H]^+$; HRMS (ESI^+) Calcd for $C_{22}H_{21}N_4O_3Te_2$ 644.9704; Found 644.9702.

Metal ion binding study by UV-vis and fluorescence spectroscopy.

Chemosensor **NBDTe** (30 μM) was added with different metal ions (150 μM). All spectra were measured in 1.0 mL CH_3CN -water (v/v = 4:1) solutions. The light path length of cuvette was 1.0 cm.

The pH dependence on Hg^{2+} binding in chemosensor NBDTe studied by fluorescence spectroscopy.

Chemosensor **NBDTe** (30 μM) was added with Hg^{2+} (150 μM) in 1.0 mL CH_3CN -water (v/v = 4:1) solutions. The buffers were: pH 4.0 ~10.0 phosphate buffered saline (PBS).

Determination of the binding stoichiometry and the stability constants K_a of Hg(II) binding in chemosensor NBDTe.

The binding stoichiometry of **NBDTe** -Hg^{2+} complexes was determined by Job's plot experiments. The emission at 525 nm was plotted against molar fraction of **NBDTe** under a constant total concentration. The total concentration of sensor and Hg^{2+} ion was 200 μM. The molar fraction at maximum emission intensity represents the binding stoichiometry of the **NBDTe**-Hg^{2+} complexes. The maximum emission intensity was reached at a molar fraction of 0.5. The association constants K_a of **NBDTe**-Hg^{2+} complexes were determined by the Benesi–Hilderbrand equation [18]:

$$1/\Delta F = 1/\Delta F_{sat} + 1/(\Delta F_{sat}\, K_a[Hg^{2+}]) \quad (1)$$

where ΔF is the fluorescence intensity difference at 525 nm and ΔF_{sat} is the maximum fluorescence intensity difference at 525 nm. The association constant K_a was evaluated graphically by plotting $1/\Delta F$ against $1/[Hg^{2+}]$. Data were linearly fitted according to eqn (1) and the K_a value was obtained from the slope and intercept of the line.

Computational methods

Quantum chemical calculations based on density functional theory (DFT) were carried out using a Gaussian 09 program. The ground-state structures of **NBDTe** and

NBDTe–Hg^{2+} complexes were computed using the density functional theory (DFT) method with the hybrid-generalized gradient approximation (HGGA) functional B3LYP. The 6-31G basis set was assigned to nonmetal elements (C, H, N, B, and F). For the **NBDTe** and the **NBDTe**–Hg^{2+} complex, the LanL2DZ basis set was used for Te and Hg^{2+}, whereas the 6-31G basis set was used for other atoms.

Cell Culture

The cell line RAW 264.7 cells were provided by the Food Industry Research and Development Institute (Taiwan). The RAW 264.7 cells were grown in DMEM supplemented with 10% FBS at 37 °C and 5% CO_2. Cells were plated on 14 mm glass coverslips and allowed to adhere for 24 h.

Cytotoxicity assay

The methyl thiazolyl tetrazolium (MTT) assay was used to measure the cytotoxicity of **NBDTe** in RAW 264.7 cells. RAW 264.7 cells were seeded into a 96-well cell-culture plate. Various concentrations (10, 15, 25 μM) of **NBDTe** were added to the wells. The cells were incubated at 37 °C under 5% CO_2 for 24 h. 10 mL MTT (5 mg ml^{-1}) was added to each well and incubated at 37 °C under 5% CO_2 for 4 h. The MTT solution was removed and yellow precipitates (formazan) observed in plates were dissolved in 200 mL DMSO and 25 mL Sorenson's glycine buffer (0.1 M glycine and 0.1 M NaCl). A Multiskan GO microplate reader was used to measure the absorbance at 570 nm for each well. The viability of cells was calculated according to the following equation:

Cell viability (%) = (mean of absorbance values of the treatmentgroup)/(mean of absorbance values of the control group).

Fluorescence Imaging

RAW 264.7 cells were cultured in Dulbecco's modied Eagle's medium (DMEM) supplemented with 10% fetal bovine serum (FBS) at 37 °C under an atmosphere of

5% CO_2. Cells were plated on 14 mm glass coverslips and allowed to adhere for 24 h. Experiments to assess the Hg^{2+} uptake were performed in phosphate-buffered saline (PBS) with 20 μM $Hg(ClO_4)_2$. The cells were treated with 10 mM solutions of $Hg(ClO_4)_2$ (2 μL; final concentration: 20 μM) dissolved in sterilized PBS (pH = 7.4) and incubated at 37 °C for 30 min. The treated cells were washed with PBS (3×2 mL) to remove remaining metal ions. Culture medium (2 mL) was added to the cell culture, which was then treated with a 10 mM solution of chemosensor **NBDTe** (2 μL; final concentration: 20 μM) dissolved in DMSO. The samples were incubated at 37 °C for 30 min. The culture medium was removed, and the treated cells were washed with PBS (3×2 mL) before observation.

Acknowledgements

We gratefully acknowledge the financial support of Ministry of Science and Technology (Taiwan, MOST 103-2113-M-009-005).

Notes and references

[a] Department of Applied Chemistry, National Chiao Tung University, Hsinchu, Taiwan 300, Republic of China E-mail: spwu@mail.nctu.edu.tw;
Fax: +886-3-5723764; Tel: +886-3-5712121 ext. 56506

†Electronic Supplementary Information (ESI) available: ^1H and ^{13}C NMR spectra of bis(2-(phenyltellanyl)ethyl) amine, ^1H and ^{13}C NMR spectra of chemosensor **NBDTe**, calibration curve of **NBDTe** with Hg(II). See DOI: 10.1039/b000000x/

1 E. M. Nolan and S. J. Lippard, *Chem. Rev.,* 2008, **108**, 3443–3480.

2 H. N. Kim, W. X. Ren, J. S. Kim and J. Yoon, *Chem. Soc. Rev.,* 2012, **41**,3210–3244.

3 H. H. Harris, I. J. Pickering and G. N. George, *Science*, 2003, **301**, 1203.

4 C. H. Lamborg, C. R. Hammerschmidt, K. L. Bowman, G. J. Swarr, K. M. Munson, D. C. Ohnemus, P. J. Lam, L. Heimburger, M. J. A. Rijkenberg and M. A. Saito, *Nature,* 2014, **512**, 65-68.

5 M. Harada, *Crit. Rev. Toxicol.,* 1995, **25**, 1–24.

6 Y. Gao, S. De Galan, A. De Brauwere, W. Baeyens and M. Leermakers, *Talanta,* 2010, **82**, 1919–1923.

7 F. Moreno, T. Garcia-Barrera and J. L. Gomez-Ariza, *Analyst*, 2010, **135**,

2700–2705.
8 X. Chai, X. Chang, Z. Hu, Q. He, Z. Tu and Z. Li, *Talanta*, 2010, **82**, 1791–1796.
9 X. Fu, X. Chen, Z. Guo, C. Xie, L. Kong, J. Liu and X. Huang, *Anal. Chim. Acta*, 2011, **685**, 21-28.
10 B. N. Ahamed and P. A. Ghosh, *Dalton Trans.*, 2011, **40**, 12540-12547.
11 D. Kim, K. Yamamoto, K. H. Ahn, *Tetrahedron*, 2012, **68**, 5279-5282.
12 X. Ma, J. Wang, Q. Shan, Z. Tan, G. Wei, D. Wei and Y. Du, *Org. Lett.,* 2012, **14**, 820–823.
13 M. Vedamalai and S. Wu, *Org. Biom. Chem.,* 2012, **10**, 5410-5416.
14 Z. Dong, X. Tian, Y. Chen, J. Hou and J. Ma, *RSC Adv.,* 2013, **3**, 2227–2233.
15 A. K. Atta, S. B. Kim, J. Heo and D. G. Cho, *Org. Lett.,* 2013, **15**, 1072–1075.
16 Y. Mikata, F. Nakagaki and K. Nakanishi, *New J. Chem.,* 2013, **37**, 2236-2240
17 S. Yu and S. Wu, *Sens. Actuators B,* 2014, **201**, 25-30.
18 K. Ghosh, D. Tarafdar, A. Samadder and A. R. Khuda-Bukhsh, *New J. Chem.*, 2013, **37**, 4206-4213
19 S. Madhu, S. Josimuddin and M. Ravikanth, *New J. Chem.,* 2014, **38**, 3770-3776
20 H. Jiang, J. Jiang, J. Cheng, W. Dou, X. Tang, L. Yang, W. Liu and D. Bai, *New J. Chem.,* 2014, **38**, 109--114
21 D. S. McClure, *J. Chem. Phys.,* 1952, **20**, 682-686.
22 H. A. Benesi and J. H. Hildebrand, *J. Am. Chem. Soc.,* 1949, **71**, 2703–2707.

Figure and scheme captions

1. **Scheme 1.** Synthesis of chemosensor **NBDTe**
2. **Scheme 2.** Energy diagram for the reaction of **NBDTe** with Hg^{2+}.
3. **Fig. 1.** (a) Color and (b) fluorescence photographs of **NBDTe** (30 μM) in acetonitrile-water (v/v = 4:1) solutions.
4. **Fig. 2.** Fluorescence response of chemosensor **NBDTe** (30 μM) in the presence of Hg^{2+} and other metal ion (150 μM) in acetonitrile-water (v/v = 4:1) solutions. The excitation wavelength was 463 nm.
5. **Fig. 3.** Fluorescence response of chemosensor **NBDTe** (30 μM) to various equivalents of Hg^{2+} in acetonitrile-water (v/v = 4:1) solutions. The excitation wavelength was 463 nm.
6. **Fig. 4.** Fluorescence response of chemosensor **NBDTe** (30 μM) to Hg^{2+} (150 μM) or 150 μM of other metal ions (the black bar portion) and to the mixture of other metal ions (150 μM) with Hg^{2+} (150 μM) (the red bar portion) in acetonitrile-water (v/v = 4:1) solutions
7. **Fig. 5.** Job plot of the Hg^{2+}- **NBDTe** complexes in an acetonitrile-water (v/v = 4:1) solution. The total concentration of **NBDTe** and Hg^{2+} was 200.0 μM. The monitored wavelength was 463 nm.
8. **Fig. 6.** Binding constant for titration of Hg^{2+} (0.1 to 1.0 eq) against ratio of fluorescence response for **NBDTe** (30.0 μM) in CH_3CN/H_2O (v/v = 4:1). The excitation wavelength was 463 nm. The binding constant was 3.81×10^3 M^{-1} of **NBDTe** for binding Hg^{2+}.
9. **Fig. 7.** ^1H NMR (300 MHz) spectra of **NBDTe** (25 mM) upon titration with (a) 0 equiv, (b) 0.5 equiv, (c) 1.0 equiv, (d) 2.0 equiv, (e) 3.0 equiv of Hg^{2+} in DMSO- d_6.
10. **Fig. 8**. Fluorescence response (532 nm) of free chemosensor **NBDTe** (30.0 μM) (□) and after addition of Hg^{2+} (450.0 μM) (■) in CH_3CN/H_2O (v/v = 4:1, 1 mM PBS buffer) solution as a function of different pH values. The excitation wavelength was 463 nm.
11. **Fig. 9.** Front views of predicted structures of **NBDTe** and **NBDTe** -Hg^{2+} complexes with B3LYP/LanL2DZ method.
12. **Fig. 10.** Reversible binding of Hg^{2+} to **NBDTe**. Fluorescence spectra of (a) **NBDTe**, (b) **NBDTe** in the presence of Hg^{2+}(90 μM), and (c) **NBDTe** in the presence of Hg^{2+} (90 μM) upon addition of Na_2S (360 μM).
13. **Fig. 11.** MTT assay of RAW 264.7 cells were treated in the presence of **NBDTe** (0 – 25 μM) incubated at 37 °C for 24 hours.
14. **Fig. 12.** Fluorescence images of RAW 264.7 cells treated with **NBDTe** and Hg^{2+}. (Left) Bright field image; (middle) fluorescence image and (right) merged image.

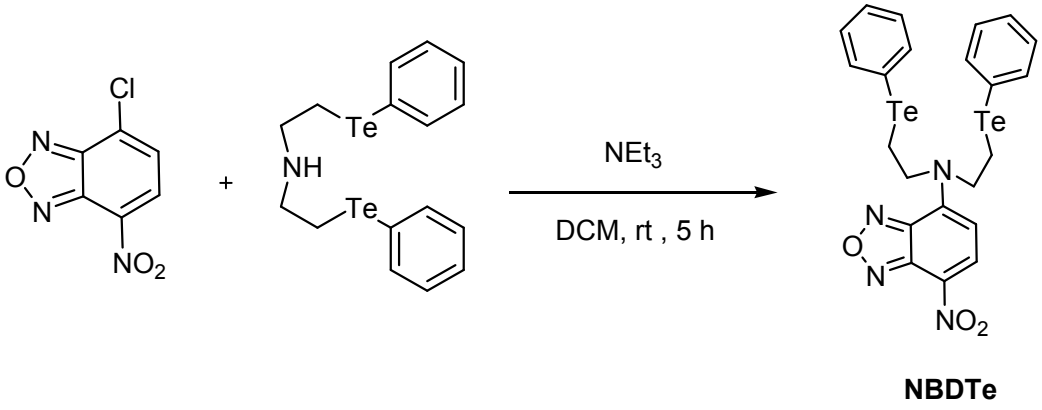

Scheme 1. Synthesis of chemosensor **NBDTe**

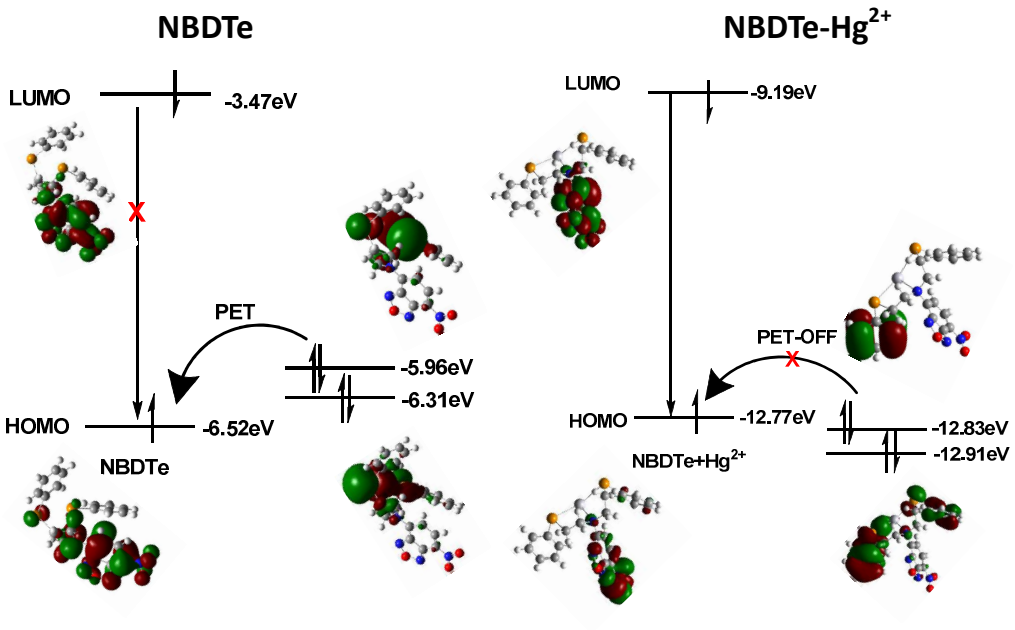

Scheme 2. Energy diagram for the reaction of **NBDTe** with Hg^{2+}.

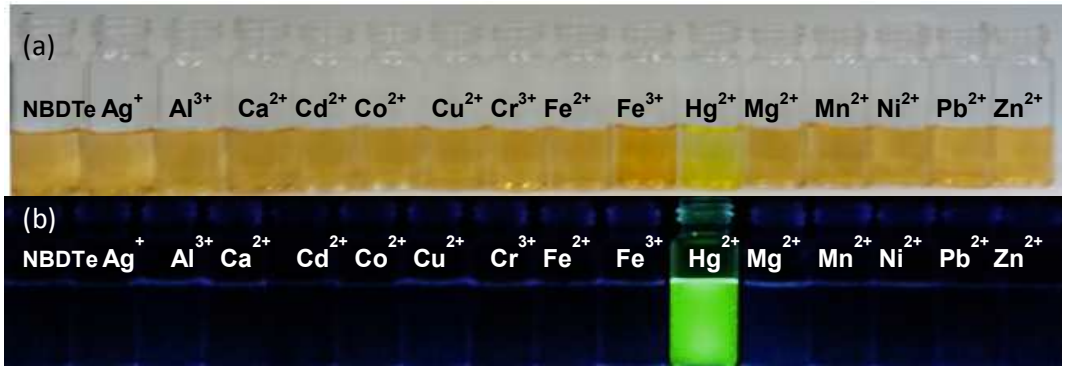

Fig. 1. (a) Color and (b) fluorescence photographs of **NBDTe** (30 μM) in acetonitrile-water (v/v = 4:1) solutions.

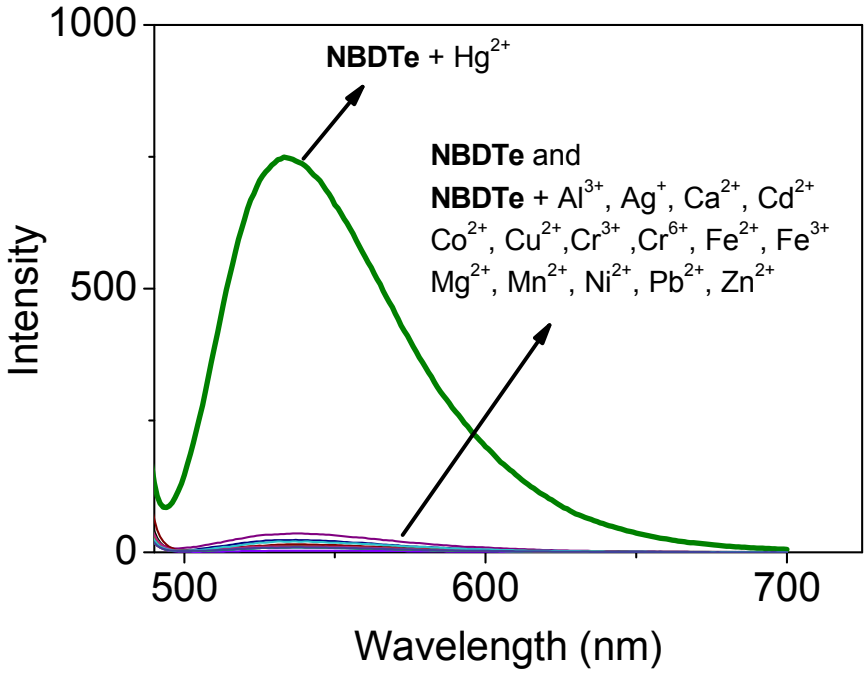

Fig. 2. Fluorescence response of chemosensor **NBDTe** (30 μM) in the presence of Hg^{2+} and other metal ion (150 μM) in acetonitrile-water (v/v = 4:1) solutions. The excitation wavelength was 463 nm.

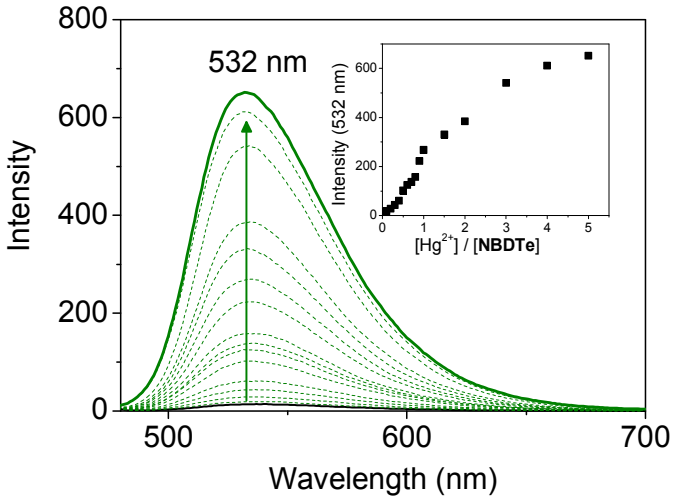

Fig. 3. Fluorescence response of chemosensor **NBDTe** (30 μM) to various equivalents of Hg^{2+} in acetonitrile-water (v/v = 4:1) solutions. The excitation wavelength was 463 nm.

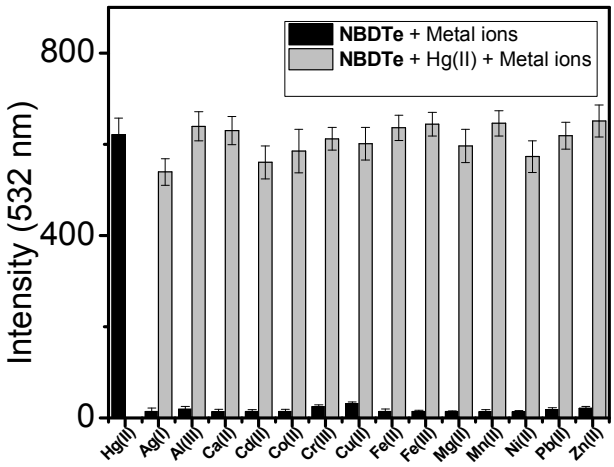

Fig. 4. Fluorescence response of chemosensor **NBDTe** (30 μM) to Hg^{2+} (150 μM) or 150 μM of other metal ions (the black bar portion) and to the mixture of other metal ions (150 μM) with Hg^{2+} (150 μM) (the red bar portion) in acetonitrile-water (v/v = 4:1) solutions

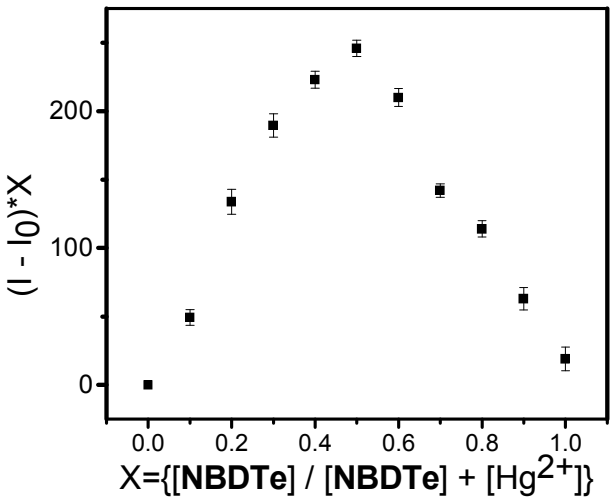

Fig. 5. Job plot of the Hg^{2+}- **NBDTe** complexes in an acetonitrile-water (v/v = 4:1) solution. The total concentration of **NBDTe** and Hg^{2+} was 200.0 μM. The monitored wavelength was 463 nm.

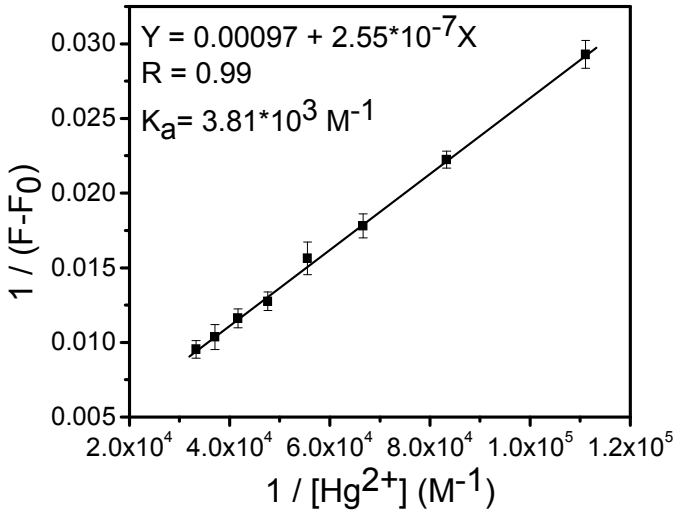

Fig. 6. Binding constant for titration of Hg^{2+} (0.1 to 1.0 eq) against ratio of fluorescence response for **NBDTe** (30.0 μM) in CH_3CN/H_2O (v/v = 4:1). The excitation wavelength was 463 nm. The binding constant was 3.81×10^3 M^{-1} of **NBDTe** for binding Hg^{2+}.

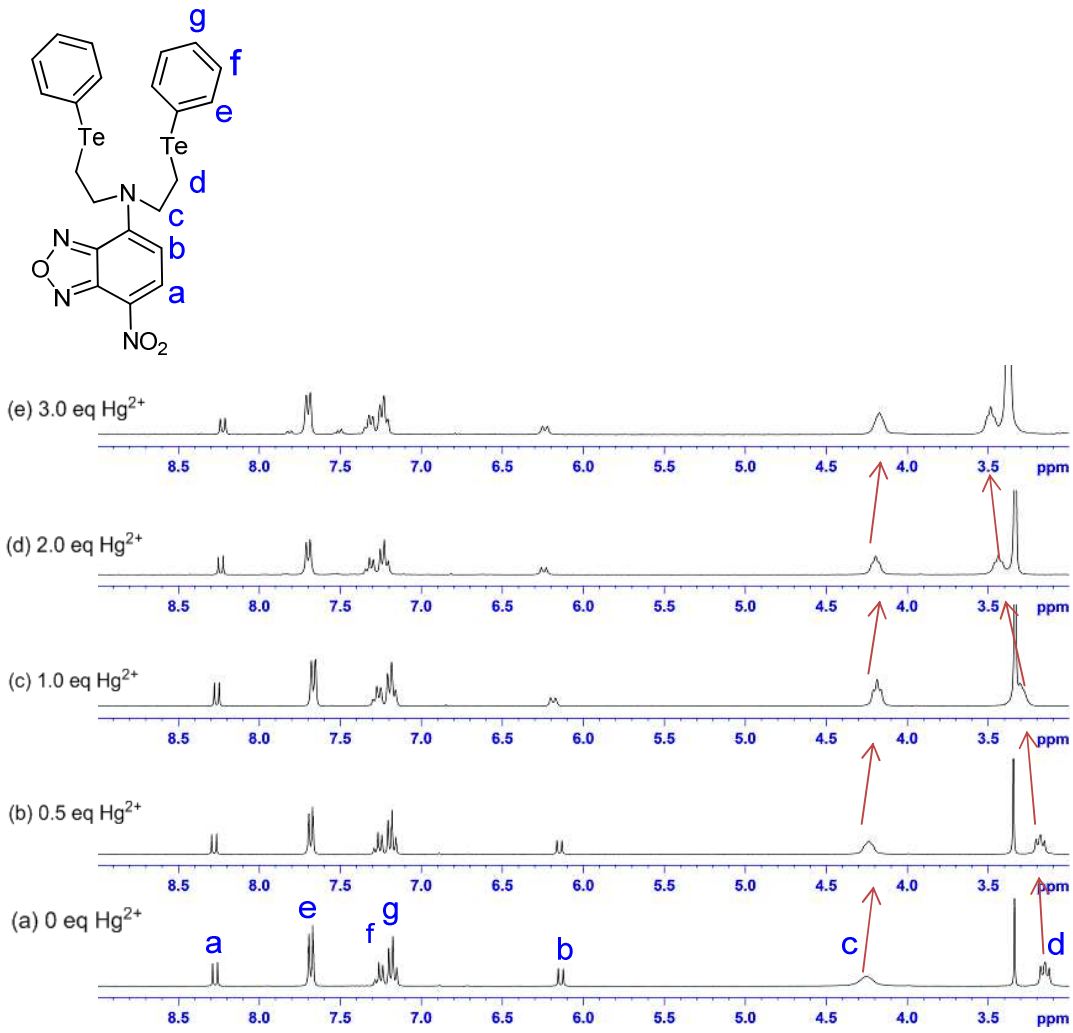

Fig. 7. ^{1}H NMR (300 MHz) spectra of **NBDTe** (25 mM) upon titration with (a) 0 equiv, (b) 0.5 equiv, (c) 1.0 equiv, (d) 2.0 equiv, (e) 3.0 equiv of Hg^{2+} in DMSO- d_6.

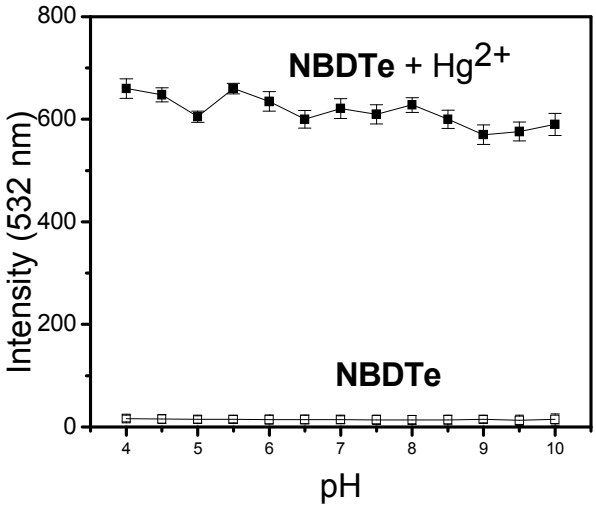

Fig. 8. Fluorescence response (532 nm) of free chemosensor **NBDTe** (30.0 μM) (□) and after addition of Hg^{2+} (450.0 μM) (■) in CH_3CN/H_2O (v/v = 4:1, 1 mM PBS buffer) solution as a function of different pH values. The excitation wavelength was 463 nm.

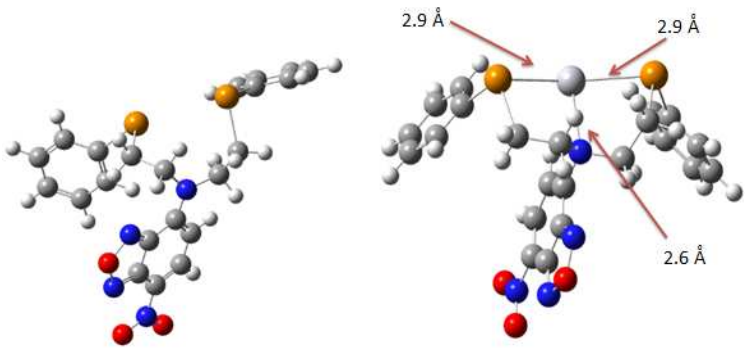

Fig. 9. Front views of predicted structures of **NBDTe** and **NBDTe** -Hg^{2+} complexes with B3LYP/LanL2DZ method.

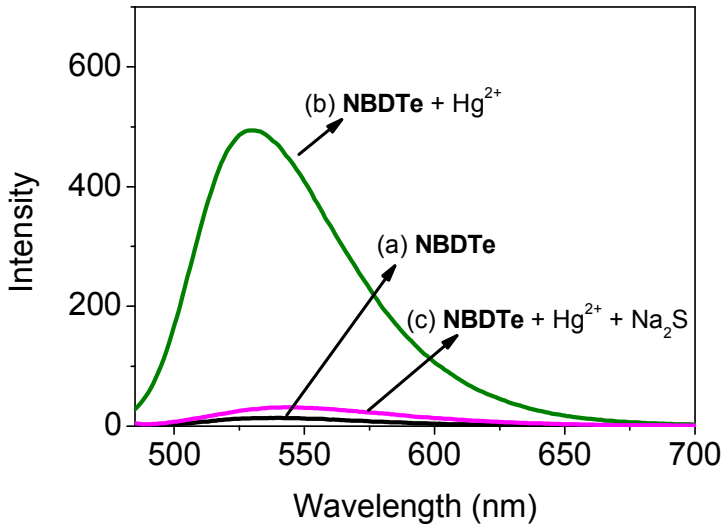

Fig. 10. Reversible binding of Hg^{2+} to **NBDTe**. Fluorescence spectra of (a) **NBDTe**, (b) **NBDTe** in the presence of Hg^{2+}(90 μM), and (c) **NBDTe** in the presence of Hg^{2+} (90 μM) upon addition of Na_2S (360 μM).

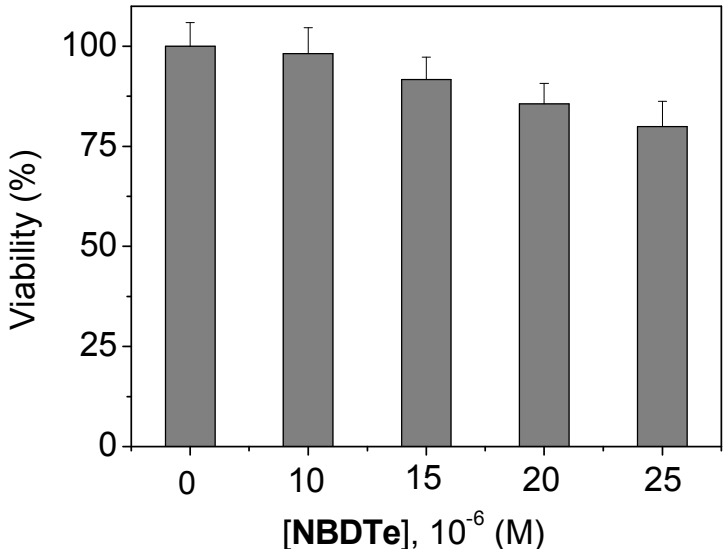

Fig. 11. MTT assay of RAW 264.7 cells were treated in the presence of **NBDTe** (0 – 25 μM) incubated at 37 °C for 24 hours.

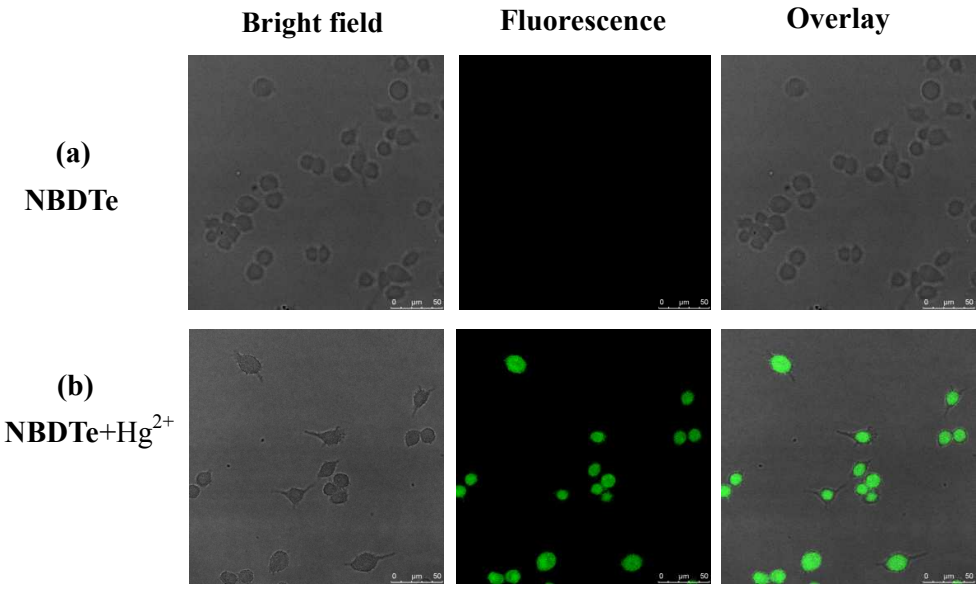

Fig. 12. Fluorescence images of RAW 264.7 cells treated with **NBDTe** and Hg^{2+}. (Left) Bright field image; (middle) fluorescence image and (right) merged image.